Open Archive Toulouse Archive Ouverte

OATAO is an open access repository that collects the work of Toulouse researchers and makes it freely available over the web where possible

This is an author's version published in: http://oatao.univ-toulouse.fr/25706

Official URL:

https://doi.org/10.1115/1.4045024

Any correspondence concerning this service should be sent to the repository administrator: tech-oatao@listes-diff.inp-toulouse.fr

A. Degeneve
Laboratoire EM2C,
CNRS, CentraleSupélec,
Université Paris-Saclay,
8-10, rue Joliot Curie,
Gif-sur-Yvette Cedex 91192, France;
Air Liquide, Centre de recherche Paris Saclay,
Chemin de la Porte des Loges,
B.P. 126,
Les Loges en Josas 78354, France
e-mail: arthur.degeneve@centralesupelec.fr

C. Mirat
Laboratoire EM2C,
CNRS, CentraleSupélec,
Université Paris-Saclay,
8-10, rue Joliot Curie,
Gif-sur-Yvette Cedex 91192, France

J. Caudal
Air Liquide, Centre de recherche Paris Saclay,
Chemin de la Porte des Loges,
B.P. 126,
Les Loges en Josas 78354, France

R. Vicquelin
Laboratoire EM2C,
CNRS, CentraleSupélec,
Université Paris-Saclay,
8-10, rue Joliot Curie,
Gif-sur-Yvette Cedex 91192, France

T. Schuller
Laboratoire EM2C,
CNRS, CentraleSupélec,
Université Paris-Saclay,
8-10, rue Joliot Curie,
Gif-sur-Yvette Cedex 91192, France;
Institut de Mécanique des Fluides de
Toulouse (IMFT),
Université de Toulouse,
CNRS,
Toulouse 31400, France

Effects of Swirl on the Stabilization of Non-Premixed Oxygen-Enriched Flames Above Coaxial Injectors

An experimental study is carried out to analyze the effects of swirl on the structure and stabilization of methane non premixed oxygen enriched flames above a coaxial injector in which the two streams are eventually swirled. The mean position of the flame and the liftoff height above the injector lips are investigated with OH* chemiluminescence images. The oxygen enrichment, the momentum flux ratio between the two coflows, the swirl level inside the central jet, and the swirl level in the annular jet are varied over a large range of operating conditions. It is found that, in the absence of swirl in the central stream, the flame is always attached to the lips of the internal injection tube. As the inner swirl level increases, the flame front located at the lips of the internal injection tube dis appears. When the annular swirl level is high enough to create a central recirculating bubble, the flame detaches from the nozzle rim and remains lifted at a finite distance above the injector. Increasing the oxygen concentration shifts this transition to smaller momentum flux ratios and smaller annular swirl levels. The liftoff distance can be finely tuned and depends on the inner and outer swirl levels, and on the momentum flux ratio between the two coaxial streams. It is shown that this feature depends neither on the con finement of the injector nor on the thermal stress exerted by the hot burnt gases on the injector back plane. About 1000 configurations were investigated that could be classified into only four distinct stabilization modes, in which the flame structure was shown to fol low a similar pathway when the momentum flux ratio between the two streams, the swirl level in the central and external streams, and the quarl angle of the annular stream are varied. It is finally shown how these limits are altered when the oxygen concentration in the annular oxidizer stream is varied from air to oxygen enriched operation.

1 Introduction

Flame stabilization above an injector nozzle is one of the main critical issues for the lifespan of the burner. The injecting device must not only provide proper conditions for the combustion pro cess but also limit the thermal stress imparted to the burner. In many non premixed systems, separation of the reactants is achieved by placing an inner fuel tube inside the oxidizer stream. Flame attachment is in this case favored in the wake of the metal lic injector components, which are submitted to high temperatures and high thermal loads. This issue is particularly salient for oxy combustion operations, in which cases the high reactivity of the mixture promotes flame attachment that may damage the injector [1].

Oxy combustion has already proven its economic viability, especially in the glass industry [2], and is currently seen as one of the most promising technology for carbon capture and storage [3,4]. Replacement of air by pure oxygen increases the flame temperature [1] and reduces fuel consumption and the volume of flue gases. In some cases, it may also be used to reduce NO_x emis sions [5,6].

Increasing the stoichiometric mixture fraction z_{st} drastically extends the extinction limits of counter flow diffusion flames [7]. The development of new technologies with oxygen enriched air leads to systems operating with highly reactive mixtures [1] and with increased stoichiometric mixture fraction values z_{st}, both leading to a better flame resistance to aerodynamic strain. These conditions favor flame attachment to the injector nozzle in non premixed conditions. One proven solution used in oxy burners in the glass industry to avoid flame attachment to the burner lip is to inject apart the fuel and the oxidizer with separated jets [8]. The length between the edge of the burner and the root of the flame, also called liftoff height, can be tuned with this type of technology [9]. However, in many systems in which space is limited, coaxial burners are preferred.

Controlling the liftoff height above coaxial injectors operating in the turbulent regime has been the topic of many investigations. The liftoff mechanism has been explained by the extinction of laminar flamelets [10], the formation of turbulent fully premixed

flames [11,12], or with the apparition of triple flames [13], which has led to the edge flame theory [14,15]. It is now established that edge flames play a fundamental role in non premixed lifted flames [16,17]. This theory implies a certain degree of premixing at the root of the flame accounting for flame propagation. In this descrip tion of the liftoff phenomenon, it is commonly assumed that the coflow velocity remains low and therefore does not play a major role in flame attachment and flame liftoff. However, Brown et al. [18] reported that a minor change in the air coflow velocity $u_{z,2}$ ($u_{z,2} = 2\,\mathrm{m\,s^{-1}}$) already alters the trends established compared to a jet flames issuing in quiescent air. The same observations were recently reported for turbulent jet flames exhausting in a high pressure vessel [19].

In many previous investigations, the coflow velocity of the oxi dizer stream remains small. For air powered injectors, lifted flames are only observed for small values of the air coflow veloc ity. Yuasa [20] could only operate his coaxial burner with air velocities $u_{z,2} < 0.5\,\mathrm{m\,s^{-1}}$ for a central methane stream and with $u_{z,2} < 8\,\mathrm{m\,s^{-1}}$ when methane is replaced by hydrogen. Above these values, the flames are blown off. It is well known that air powered flames are difficult to stabilize on a coaxial injector rim when the air velocity exceeds about $10\,\mathrm{m\,s^{-1}}$ [20 22], whereas O_2 enriched flames easily withstand these operating conditions. With the growing interest in oxy combustion, one needs to further investigate how to control flame attachment when the velocities in the oxidizer annular stream are high.

Providing a rotational motion to the annular stream of a coaxial injector is widely used to improve fuel mixing with the oxidizer [23 26]. Another well known advantage of a highly swirled flow is the formation of a central recirculation zone (CRZ), which favors flame stabilization downstream the injector thanks to the presence of low velocities and recirculation of hot burned gases [27]. The height of the stagnation point of the CRZ scales as $J^{-1/2}$ where $J = \rho_2 u_{z,2}^2 / \rho_1 u_{z,1}^2$ is the momentum flux ratio [28]. The impact of the swirl in the central fuel stream is less well docu mented. In nonreacting conditions, swirling the inner stream has been shown to push the CRZ upstream [29 31]. In reacting condi tions, Yuasa [20] made a detailed analysis of the role of the inner swirl and reported that adding a swirl motion to the central fuel stream alters the flame structure and flame stabilization. His study conducted with H_2/air and CH_4/air flames showed that adding a swirl S_1 increases the probability of liftoff and decreases the prob ability of blowoff. However, flames in Ref. [20] were only investi gated in a regime where the velocities $u_{z,2}$ in the annular stream are one order of magnitude below the inner fuel velocity $u_{z,1}$. This leads to flames dominated by the inner jet momentum in the limit $J \ll 1$.

In many industrial applications, the difference between the velocities in the central and annular streams is not that high while the velocities of the oxidizer annular stream could be high as well. These systems operate at higher values of the momentum flux ratio J typically larger than $J > 0.5$. This has motivated the current study, in which the flow injection conditions in both streams are extensively varied to unravel the main parameters controlling flame stabilization with high velocities in the annular oxidizer channel.

The article is organized as follows. The experimental setup is described in Sec. 1. Experiments are first reported without swirl in the central fuel stream in Sec. 2. The effects of the central swirl level are analyzed in Sec. 3, followed by the effects of confine ment in Sec. 4. Changes in the injector geometry are examined in Sec. 5 by modifying the quarl angle of the annular injector. The influence of the O_2 enrichment is finally investigated in Sec. 6. These experiments are used to identify the mechanisms altering flame stabilization above coaxial swirling injectors.

2 Experimental Setup

The test rig is the Oxytec combustor which has already been used to investigate the effects of swirl [32] and of the diverging cup of the burner [33] on the stabilization of technically premixed
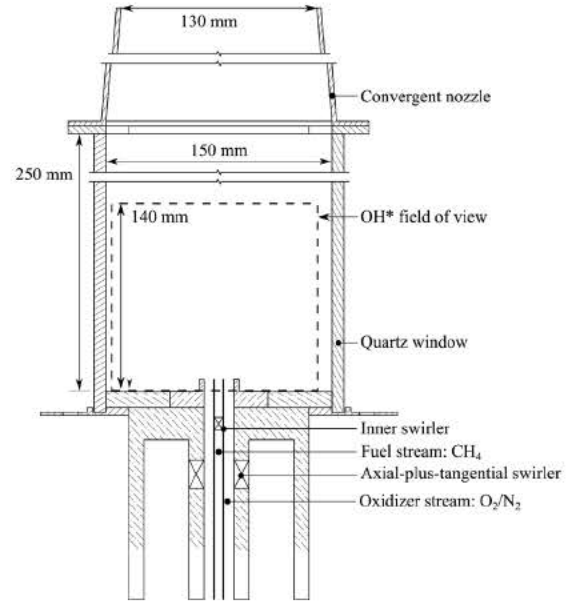

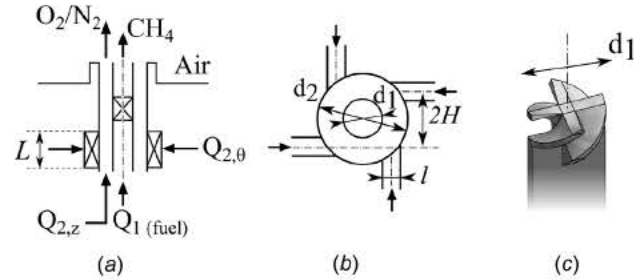**Fig. 1 Schematic of the Oxytec test rig**

Fig. 2 Sketch of the coaxial injector: (a) axial cut, (b) trans verse cut through the annular swirler, and (c) three quarter-view of the axial inner swirler

flames. The same burner without combustion chamber has also been used to examine scaling relations for length of oxy flames stabilized on coaxial injectors [26].

The combustion chamber is represented in Fig. 1, and the injec tor is sketched in Fig. 2. The injector comprises a central tube of inner diameter $d_1 = 6$ mm which conveys the methane flow and an annular channel of outer diameter $d_2 = 20$ mm filled with O_2 enriched air. The thickness of the burner lips is $e = 1$ mm. In some experiments, the annular channel eventually ends with a quarl angle α (see Fig. 3). Rotational motions are provided to both the central and the annular streams. Given the number of parameters considered in this study, it was not possible to investigate co and counter rotative swirling vanes. The choice of counter rotation is indeed as interesting as co rotation, but the latter choice is retained here. A comparison study is planned to compare co rotating and counter rotating operations. The inner stream is swirled with the help of four removable sets of axial twisted vanes with trailing edge angles $\theta_1 = 0$ deg, 30 deg, 50 deg, and 60 deg. Assuming a solid body rotation of the inner fuel stream, the geo metrical swirl number S_1 is given by $S_1 = 1/2 \tan(\theta_1) = 0$, 0.29, 0.60, and 0.87. Each swirler is composed of four blades which cover the whole cross section area with a slight overlap as illus trated in Fig. 2(c). The inner swirler is set with a recess of $2d_1$ upstream the injection plane. The swirling motion in the annular oxidizer stream is generated with four tangential slits as shown in Fig. 2(b). The distribution of the axial $Q_{2,z}$ and tangential $Q_{2,\theta}$ vol ume flowrates provides an adjustable swirl level S_2 that can be var ied during operation of the injector (Fig. 2(a)). With the same
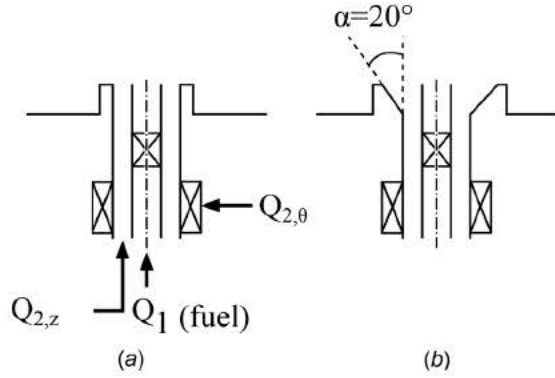
Fig. 3 Sketch of the injector with and without diverging cup

solid body rotation hypothesis on the structure of the annular flow, the geometrical swirl number S_2 in the annular channel is given by

$$S_2 = \frac{\pi H d_2}{4 N l L} \frac{1}{1 + Q_{2,z}/Q_{2,\theta}} \frac{(d_1/d_2)^4}{} \quad (1)$$

where $H = 9$ mm is the distance separating the tangential injection channels from the burner axis, $l = 3$ mm the width, and $L = 10$ mm the height of the $N = 4$ tangential injection channels regularly distributed around the circumference of the outer tube (see Fig. 2(b)). This system provides an outer swirl number S_2 ranging from 0 up to 1.23. The inner fuel stream and the oxidizer annular stream are mixed downstream the injector, in the combustion chamber whose main dimensions are given in Fig. 1. The injection plane of the coaxial injector is located 5 mm above the back plane of the combustor to ease imaging the flame root and flame liftoff height. This height defines the axial origin $z = 0$, and there is no recess between the central and the outer injection tube outlets.

Most experiments are conducted with an oxygen mass fraction set to $Y_{O_2,2} = 0.40$ in the oxidizer stream. The effects of the O_2 enrichment are examined in Sec. 6, in which it is varied from $Y_{O_2,2} = 0.23$ to simulate air powered flames to $Y_{O_2,2} = 0.50$. Higher oxygen levels could not be reached with this setup.

Flame shapes and liftoff characteristics are investigated over a large range of operating conditions. One can attempt the following dimensional analysis. The axial and tangential mass flow rates, the pressure, the preheat temperature of the reactants, and the geometry of the combustion chamber can be gathered in dimensionless numbers that describe the aerodynamics of the flow. This leads to define a Reynolds number $Re_2 = \rho_2 u_{z,2} D_h / \mu_2$ based on the hydraulic diameter $D_h = 12$ mm of the annular injection channel, the momentum flux ratio $J = \rho_2 u_{z,2}^2 / \rho_1 u_{z,1}^2$, two swirl numbers $S_1 = 1/2 \tan(\theta_1)$ and S_2 given by Eq. (1), a confinement ratio C_r defined in Sec. 4, and the quarl opening angle α of the diffuser. The influence of the aerodynamics on flame attachment constitutes the motivation of this study. Among the physical parameters, the pressure, the temperature of the preheated reactants, and the level of O_2 enrichment also modify the chemistry, which can be related to a Damköhler number $Da = \tau_t / \tau_c$ where τ_t is a turbulent characteristic time scale and τ_c is a chemical time scale estimated by $\tau_c = \delta_l / S_L$ where δ_l and S_L are, respectively, the flame thickness and the laminar burning velocity of a one dimensional premixed flame at stoichiometry. The Damköhler numbers have been computed for CH_4/air flames ranging from ambient conditions to gas turbine operations. The effects of O_2 enrichment have also been computed at ambient conditions. It results that pressure, preheating temperature and O_2 enrichment drastically increase the Damköhler number. For practical reasons, the influence of chemistry kinetic on flame attachment is therefore approximated in this study by varying the O_2 enrichment in the oxidizer annular stream. This enables to vary the Damkölher number over about one order of magnitude at ambient conditions.

The dimensionless numbers controlling the aerodynamics are extensively varied in this study. The inner swirl number S_1 and outer swirl number S_2 both span regimes without and with vortex breakdown. The momentum flux ratio J between the annular and central jets is varied by changing the axial inner fuel velocity $u_{z,1}$. The axial velocity in the annular oxidizer stream $u_{z,2}$ remains fixed to $u_{z,2} = 15$ m s^{-1} in these experiments. This sets the annular flow in the turbulent regime with an outer Reynolds number $Re_2 = 12,000$. The thermal power P and the global equivalence ratio ϕ do not depend on S_1 nor S_2 but are correlated with J, varying from $P_{min} = 6.6$ kW and $\phi_{min} = 0.28$ when $J = 8$ up to $P_{max} = 22$ kW and $\phi_{max} = 0.9$ when $J = 0.75$. Tests, not shown here, have been carried out to determine the influence of the outer Reynolds number Re_2, which is proportional to the thermal power P, for a fixed momentum flux ratio J. In most of the explored cases, increasing Re_2 from 12,000 to 20,000 does not change the flame topology. The topologies detected are altered by the Reynolds number only for small values.

In the following experiments, the non premixed flames are designated as either attached to the injector rim or lifted further downstream. There is, however, a range of operating conditions in which the flame can be intermittently stabilized in both regimes. This work does not aim at studying this hysteresis phenomenon [20], which is not desirable from an industrial perspective. Choice is made here to designate the flames as attached if they lie in the dual state regime. This is done by always starting the burner in a regime where the flame is attached to the injector rim. The flow meters are then progressively tuned to reach the desired point of interest. The lifted flames presented in this work are therefore the ones which cannot lie in the attached regime. OH* images are recorded with an ICCD camera with a bandpass filter centered on $\lambda = 310 \pm 5$ nm. Images are focused on an axial plane crossing the burner axis and the recording time $\Delta t = 30$ ms is long compared to the largest turbulent time scales of the flow. Images are averaged with 100 snapshots. The Otsu thresholding method [34] is chosen to infer the flame front location from OH* images [35] as in Ref. [26]. The liftoff height L_f is determined as the lowest point of the Otsu contour. A sensitivity analysis has been carried out to examine changes of L_S when varying the image brightness and contrast. Different exposure times and camera apertures were tested. It appears that the largest variations of L_f are limited to within 5%.

3 Flame Stabilization Without Inner Swirl

The flame topologies are first examined without swirl $S_1 = 0$ in the central fuel stream by removing the axial swirling vane. The momentum flux ratio is varied from $J = 0.75$ to 8 and the annular swirl number S_2 from 0 to 1.1. It turns out that all these flames can be stabilized on the injector without being blown off. This feature is attributed to the high resistance to strain of the O_2 enriched flames.

Nine selected flames are presented in Fig. 4 with three different outer swirl numbers $S_2 = 0.6$, 0.8, and 1 and three momentum flux ratios $J = 8$, 3, and 1. In the absence of outer swirl $S_2 = 0$, the flames feature a jet like shape. When S_2 increases, the flame shortens and the opening angle of the reaction zone widens, resulting in the formation of a stable CRZ as depicted in Fig. 4 for $S_2 = 1$. The appearance of the central vortex bubble depends on the values of both J and S_2, in compliance with the results of Chen and Driscoll [28].

When the momentum flux ratio J increases, the flame becomes more compact due to two distinct mechanisms. First, increasing the annular stream velocity compared to the central one enhances turbulent mixing between the reactants, which diminishes the length needed for the fuel and air to reach stoichiometry [36]. This mechanism fully determines the length of coaxial nonswirling flames when the momentum flux ratio J is not too low [26,37]. Scaling laws obtained in this way have been shown to also well describe the length of coaxial swirling flames, provided that they
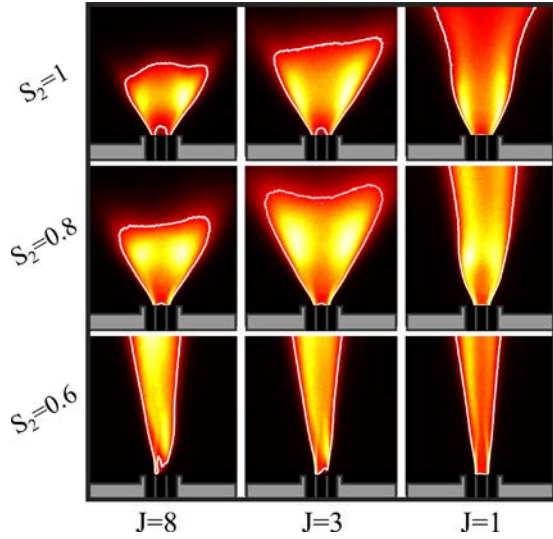
Fig. 4 OH^* flame images as a function of the momentum flux ratio J and the outer swirl number S_2. The inner swirl is fixed to $S_1 = 0$. The Otsu contour delineating the flame front location is represented in white [34]. The gray elements delineate at scale the solid components of the test rig.

remain in the jet like regime [26]. Second, when both the momentum flux ratio J and the annular swirl number S_2 are high enough, the flow field is strongly modified with the appearance of a stable CRZ that pushes the reaction zone upstream and makes the flame more compact.

All the investigated flames in this first set of experiments are well attached to the lips of the central tube. This feature is exemplified in Fig. 4 showing the OH^* emission distribution of nine selected flames. These observations remain valid for all the 91 operating conditions investigated when $S_1 = 0$, $0.75 \leq J \leq 8$ and $0 \leq S_2 \leq 1.1$. Flame images of the OH^* emission intensity collected with a short exposure time $\Delta t = 1$ μs, not shown here, always detect OH^* light close to the injector lip.

The flame front starts at the edge of the internal injector rim, which is the most upstream point where the methane and the oxidizer meet. For flames obtained with a high outer swirl number S_2, the OH^* peak emission slightly shifts radially above the oxidizer stream, as in the top row images in Fig. 4 when $S_2 = 1$. In these conditions, the CRZ lies just above the central injection tube outlet so that a small fraction of the methane stream is pushed

toward the annular channel upstream within the oxidizer flow. This yields a diffusion flame front anchored in the annular stream a few millimeters below the injection plane. This reaction taking place inside the annular channel is not visible from the view angle of Fig. 4 due to the surrounding metallic components of the burner, but is clearly visible in images taken from the top view above the injector (not shown here). Though this flame protruding inside the injector is not entirely attached, it cannot be considered lifted either. In all the experiments carried out in the absence of inner swirl $S_1 = 0$, it was not possible to lift the oxy flames with $Y_{O_2,2} = 0.40$. These flames remain attached to the injector nozzle lip. In this stabilization mode, the injector nozzle is submitted to high thermal stress.

4 Effect of S_1 on Flame Stabilization

A swirl motion is now provided to the central fuel stream with the help of one of the three axial swirling vanes placed in the central tube. The value of the inner swirl number is varied from $S_1 = 0$ to $S_1 = 0.87$ depending on the twisted vane which is used. The flames are investigated at the same operating conditions as in Sec. 2. The momentum flux ratio is varied from $J = 0.75$ to 8 and the outer swirl number S_2 from 0 to 1.1. When the swirl level in the annular oxidizer stream is small $S_2 < 0.6$, flames in the jet like regime blow off. For higher levels of annular swirl S_2, changes of flame patterns induced by an increase in the inner swirl number S_1 are presented for three pairs of values J and S_2 in Fig. 5. On the left, the OH^* signal is integrated along the line of sight. The flames feature a discernible reaction front when stabilized close to the combustor dump plane. This enables to perform a reliable Abel deconvolution of the signal to get the OH^* distribution in an axial plane crossing the burner axis. These Abel deconvoluted images help to better estimate the flame front position and are presented on the right in Fig. 5.

When an inner swirl $S_1 > 0$ is imparted to the central flow, the flames are not all attached to the central injector nozzle anymore. In many cases, the reaction layer stabilized at the edge of the central fuel tube disappears and the flame is stabilized further downstream from the injector nozzle outlet. The selected set of images depicted in Fig. 5 points out that different values of S_1 are needed to lift the flames depending on both the values of the momentum flux ratio J and the outer swirl number S_2. At the top in Fig. 5, the outer swirl number is high $S_2 = 0.85$. For this annular swirl level, the only lifted flame is the one featuring the highest inner swirl number $S_1 = 0.87$. In the bottom row in Fig. 5, when the outer swirl is reduced to $S_2 = 0.65$ and the momentum flux is high in
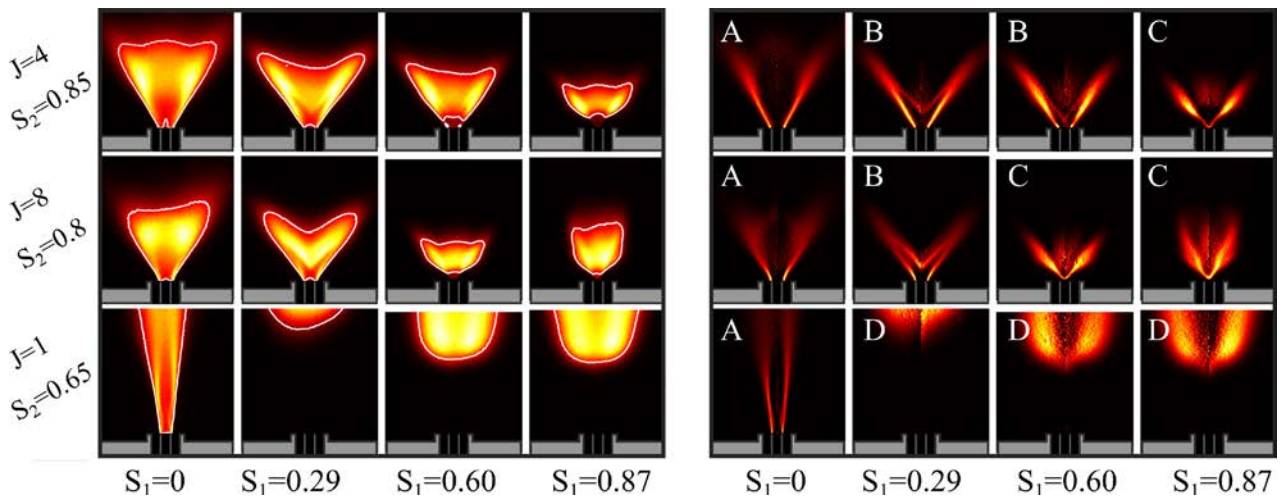
Fig. 5 OH^* flame images as a function of the inner swirl number S_1 for three selected values of the momentum flux ratio J and the outer swirl number S_2. Left: line of sight integrated images; the Otsu contour [34] is represented in white. Right: deconvoluted fields of the corresponding left images with Abel transform.
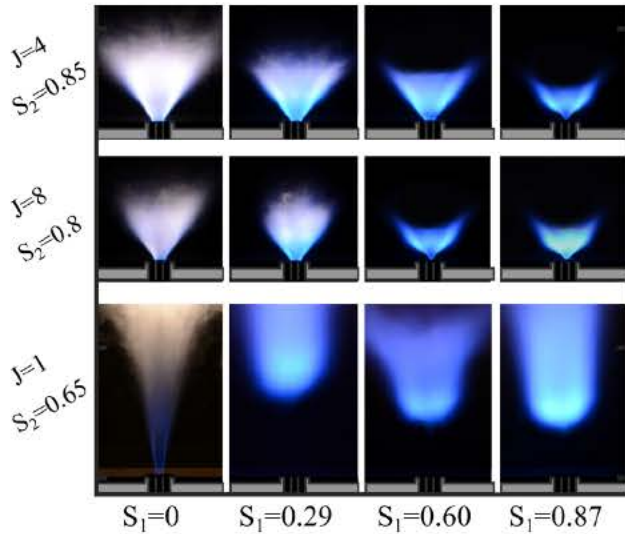
Fig. 6 Averaged flames images in the visible spectrum as a function of the inner swirl number S_1 for three selected values of the momentum flux ratio J and the outer swirl number S_2

Fig. 7 Stabilization chart with Type B and Type C topologies as sketched in Fig. 8 mapped with respect to the momentum flux ratio J and the outer swirl number S_2 for different values of the inner swirl number $S_1 = 0$, 0.29, 0.6, and 0.87. For $S_1 = 0$, the flame is always attached to the central nozzle rim.

the central stream with $J = 1$, even a small swirl level $S_1 = 0.29$ leads to a lifted flame. In this case, the flame is stabilized far away from the injector nozzle outlet at a height L_f equal to $L_f/d_1 = 8$. Though the liftoff height is large, fluctuations of the flame position remain relatively weak. These flames remain stable and are not subject to blowoff. In this regime, increasing further the value of the inner swirl number S_1 decreases the liftoff height from $L_f/d_1 = 13$ when $S_1 = 0.29$ down to $L_f/d_1 = 8$ when $S_1 = 0.87$. A similar behavior was identified in Ref. [20].

The impact of the inner swirl on the flame stabilization is now further analyzed with the help of flame images in the visible spectrum. In Fig. 6, the same set of flames is displayed as in Fig. 5. The flame averaged emission in the visible range is collected with a camera (Nikon 7000D, Sigma lens 70 300 mm) and a long exposure time $\Delta t = 1$ s. In the absence of inner swirl $S_1 = 0$, flames are in the jet like regime as in the bottom left corner in Fig. 5 and are attached to the nozzle rim. They feature a blue reaction zone at their root, but one sees that they become yellow and orange further downstream. This yellow/orange color at the flame tip indicates soot production. This is also the case for flames featuring a CRZ at top left corner in Fig. 5, even though soot production is reduced. When the inner swirl number S_1 increases, this yellow/orange signal progressively vanishes and the flames feature a deep blue color in the third and fourth rows in Fig. 5. These observations indicate that the inner swirl improves mixing for both attached and lifted flames.

The liftoff height has been determined for a large set of momentum flux ratio J and annular swirl number S_2 using the OH* images recorded along the line of sight. This yields the stabilization chart drawn in Fig. 7 delineating the operating conditions between flames attached to the central injector rim and the lifted ones. This chart has been determined for the three swirling vanes inserted in the central stream yielding increasing swirl levels S_1. It clearly appears that flame attachment independently varies with the three parameters J, S_1 and S_2. Under the covered operating conditions, a necessary condition to lift the flame is that the inner swirl number S_1 differs from zero $S_1 > 0$. This condition is, however, not sufficient, and liftoff is obtained either by increasing S_1 above a threshold level or by decreasing S_2 or J.

The fact that flame detachment highly depends on J is at variance with results from Yuasa [20]. In this study where $J \ll 1$, the author reported that the liftoff transition remains unaltered by the coflow velocity in the annular injection tube. As underlined in the introduction, this illustrates that the physics controlling flame stabilization above a coaxial injector differs when the annular
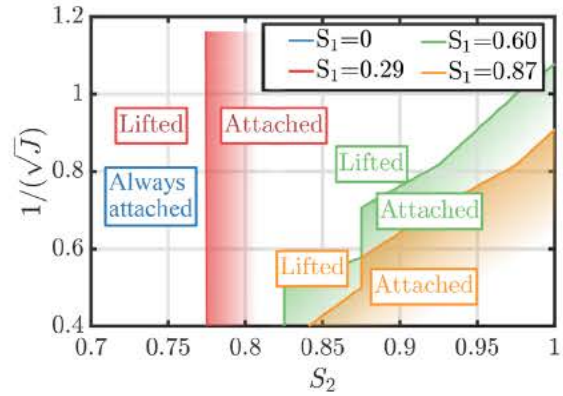
oxidizer velocity is not small compared to the central fuel velocity. One recalls that the outer swirl and inner swirl are co rotating in the present study. It is remarkable that in these conditions, swirl needs to be conferred to the central fuel flow in order to detach the flame from the central nozzle rim. This constitutes one important finding of this work. It has been verified that this feature is not due to the insertion of an obstacle in the central tube. A vane with a vanishing blade angle $\theta_1 = 0$ deg has been introduced and flames remained all attached to the injector rim in this configuration independently of the values set for J and S_2.

The position of the flame front is now analyzed in more detail with the help of the deconvoluted images on the right side in Fig. 5. As described in Sec. 2, without inner swirl $S_1 = 0$, all flames are stabilized in the jet like regime at the nozzle lip of the central injection tube as shown in Fig. 4. This stabilization mode is the same for the jet flames without annular swirl $S_2 = 0$ and for the swirled flames $S_2 > 0$. The only difference is that the opening angle of the reaction layer widens with the outer swirl number S_2. When a swirl motion $S_1 > 0$ is added to the central fuel stream, the flames feature four distinct topologies which are sketched in Fig. 8 in an axial plane through the burner:

- Type A flames are also named ring stabilized jet flames. The reaction layer is anchored on the lip of the central injector and a diffusion flame develops in the shear layer where the fuel and oxidizer streams meet at stoichiometry. These flames are stabilized in the jet like regime as in the bottom row in Fig. 4 with a round concave flame tip. They may also eventually feature a CRZ as in the top left image in Fig. 4.
- Type B flames feature two distinct reaction layers. The first reaction layer is the Type A diffusion jet flame stabilized at the rim of the central injector. This first reaction zone is completed at the top by a second reaction layer away from the injector and labeled Type C flame with a V shape. In this second reaction layer, the fuel burns with vitiated hot air. Type B flames remain anchored on the central nozzle lip.
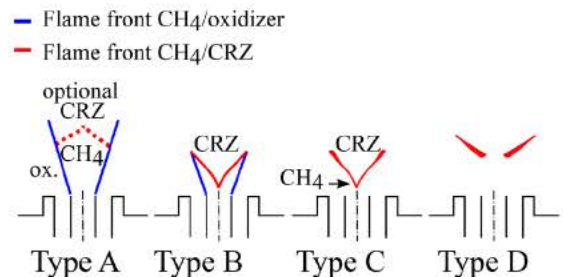

Fig. 8 Four distinct topologies of flames stabilized above the coaxial injector

- Type C flame is a flame for which the Type A diffusion jet flame front has disappeared. The reaction layer is now only located between the fuel stream and the CRZ where the recirculating hot gases and the oxidizer are mixed. Though the flame is stabilized close to the injector, the flame front is not in contact with any metallic component. The flame is therefore lifted and fully aerodynamically stabilized. In this mode, the liftoff height remains small $L_f/d_1 < 1$.
- Type D flame has the same topology as Type C flame, but it is stabilized further downstream from the injector outlet with $L_f/d_1 > 1$. As reported in Fig. 5, the liftoff height in this mode is very sensitive to the injection conditions.

Transition from Type A to Type B flames is smooth. When type A flames with $S_1 = 0$ feature a CRZ, the reaction front between methane and the CRZ is diffuse and hardy discernible (see Fig. 5). This is attributed to the momentum of the nonswirling inner jet that pushes the reaction zone downstream. For Type A flames featuring a CRZ, the flame front close to the CRZ is diffuse. Conversely, a type B flame features a bright V flame front between the methane stream and the CRZ. The higher swirl level in the inner jet favors vortex breakdown which places the CRZ more upstream. Transition from type B to type C flames is steeper. As soon as the diffusion reaction layer in the shear layer between the two coaxial streams has disappeared, the lifted V flame produces more sound and cannot return back to the type B shape without large modifications of the operating conditions.

Flames are now analyzed with both deconvoluted images to identify where the flame is stabilized and line of sight images which are more representative of the size and volume occupied by the flame. As shown in Figs. 5 and 6, the compactness of the flame is drastically impacted by the inner swirl number S_1. One must recall that the Reynolds number in the annular stream is kept fixed and equal to $Re_2 = 12,000$ in these experiments. At the top row in Fig. 5, the momentum flux ratio is $J = 4$, only the inner swirl number S_1 differs between the four flames. For these injection conditions, the thermal power $P = 9.4$ kW and global equivalence ratio $\Phi = 0.35$ are fixed. An increase in the inner swirl number S_1 sharply increases the flame compactness and decreases the flame length. It can be further seen that the gain of compactness is directly correlated with the transition from Type B to Type C regimes. This is also well illustrated in the middle row in Fig. 5 for $J = 8$ and $S_2 = 0.8$.

A complete characterization of the stabilization mechanism of these flames requires more elaborated diagnostics. At this stage, one may already attempt the following conjecture. In Type A and Type B regimes, a diffusion flame front is anchored to the central nozzle rim. When swirl is high enough, a central recirculation bubble forms in this flow. This CRZ cannot, however, settle close to the injector outlet due to burned gas acceleration produced in the central flow by the diffusion reaction layer anchored on the burner rim. When this diffusion reaction layer disappears and the flame stabilizes in Type C regime, the CRZ is no longer pushed by the burned gases and can freely protrude further upstream. This in turn largely shortens the flame length. It is worth mentioning that the inner fuel tube only provides a small amount of the total mass flow rate and axial momentum flux. In these conditions, it has been shown that even small variations of the inner swirl number have a large impact on the flame and flow patterns.

5 Effect of Confinement and Thermal Environment

It is now worth considering how confinement due to the combustion chamber sidewalls affects the flame topology. A criterion based on the confinement ratio $C_r = W^2/(\pi r_2^2)$, where $W = 150$ mm is the width of the square combustion chamber and $r_2 = 10$ mm the outer radius of the annular stream, is used to discriminate whether aerodynamics effects caused by the confinement need to be considered [38,39]. It has been shown in a former study conducted with premixed flames that the Oxytec combustion chamber operates in a free jet regime [33]. Besides, wall temperatures at the injector nozzle lip [40], along the combustion chamber back plate and in the outer recirculation zones [41,42], can also affect flame stabilization and the liftoff height by preheating the gases.

In order to verify whether the presence of the combustion chamber sidewalls is responsible for the previous observations, experiments are now carried out without any combustion chamber. The same injector is used, but the flames are stabilized in quiescent atmosphere above the same chamber back plane and at the same flow operating conditions as in Sec. 3 for a central swirl level $S_1 = 0.87$. In the absence of combustion chamber, the injection device does not heat up and remains at ambient temperature $T_0 = 293$ K, except for the tip of the inner tube. This new configuration of the burner prevents (i) the reactants from preheating (ii) the formation of an outer recirculation zone filled with hot burned gases and (iii) changes of the gas composition of the flow entrained by the annular oxidizer jet.

The results are shown in Fig. 9. Line of sight integrated OH* intensity distributions are represented for nine flames featuring different values of momentum flux ratio J and outer swirl number S_2. The gray elements delineate at scale the solid components of
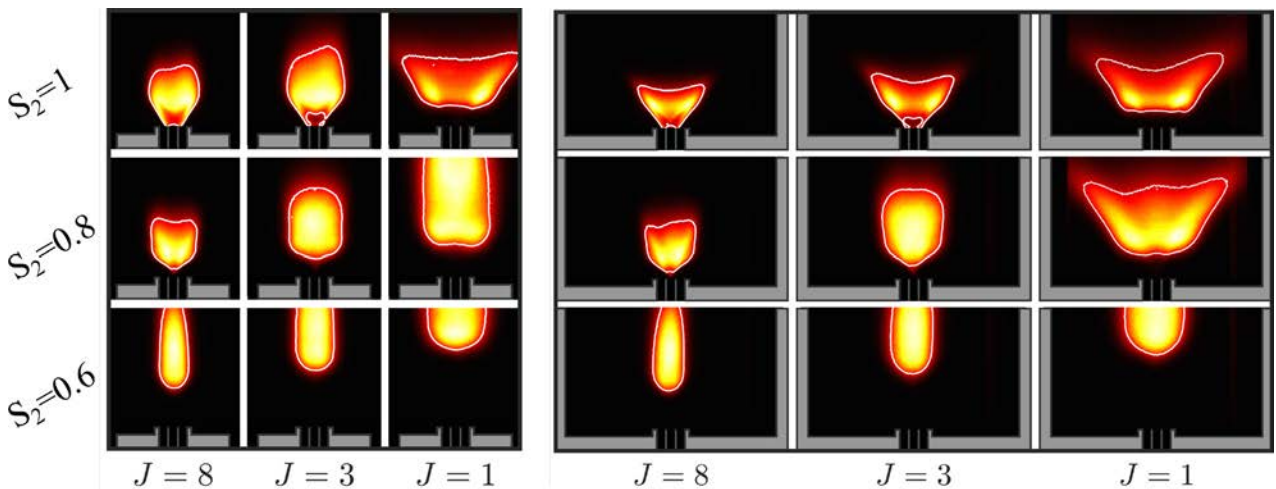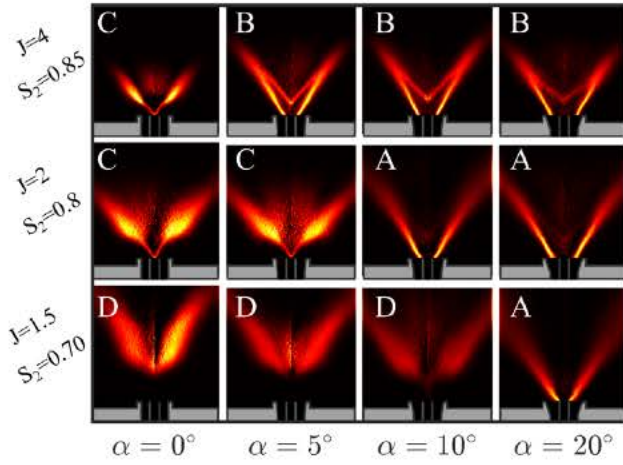

Fig. 9 OH* flame images as a function of the momentum flux ratio J and the outer swirl number S_2. S_1 0.87. Left: flames stabilized without the combustion chamber sidewalls. Right: flames stabilized inside the Oxytec combustion chamber delineated in gray.

Fig. 10 OH* flame images as a function of the quarl angle α for three selected values of the momentum flux ratio J and the outer swirl number S_2. The inner swirl number is set to S_1 0.87. Images are deconvoluted with the Abel transform. The gray elements delineate at scale the solid components of the test rig, the combustion chamber being out of the frame.

the test rig. Flames at the same operating conditions are presented without confinement on the left (the dump plane is narrow), and with confinement on the right (the lower half of the combustion chamber is represented). Though the flame topology may exhibit different behaviors downstream the central recirculation zone or at the top of the flame, the main result is that changes of the flame leading edge position are hardly discernible with or without combustion chamber. The stabilization mode of the flame does not depend on the presence of the combustion chamber. Only nine flames are presented in this figure, but the same features have been observed for a set of 60 flames covering the range of momentum flux ratio $1 \leq J \leq 8$ and outer swirl number $0.6 \leq S_2 \leq 1$. It turns out that all the flames investigated could be stabilized without the combustion chamber, and that the leading edge of the flame features exactly the same topology as the ones identified in the confined configuration. The differences are observed only further downstream the injector rim, where confinement strongly modifies the flame topology. It can be further noticed that the similarity of the flame topology with and without confinement remains excellent even for Type D flames when the liftoff height is large $L_f/d_1 = 8$ as at the bottom right corner in Fig. 9. The coaxial injector hence confers a swirling flow pattern which stabilizes the flame without being much affected by the
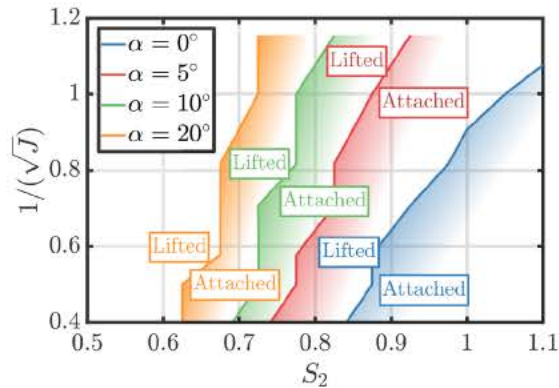
external conditions. It is therefore concluded that the impact of the confinement on the flame pattern is very limited at the root of the flame. Neither the presence of an outer recirculating flow with burned gases nor preheating of the reactants by the hot solid components of the combustor nor the gas composition of the entrained flow seem to alter flame attachment to the central nozzle lip nor the liftoff height above the injector for these air enriched flames with $Y_{O_2,2} = 0.40$.
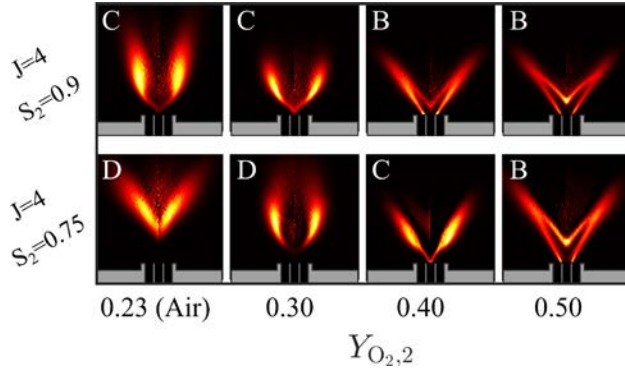
6 Effect of Quarl

The effect of replacing the straight annular injection tube by a diverging cup is analyzed in this section. As sketched in Fig. 3, the outlet section of the oxidizer annular stream is equipped with a quarl in which the cross section area is increased. The reactants are injected at the same operating conditions as in Sec. 3. Choice has been made to keep the same definition for the momentum flux ratio J and the outer swirl number S_2, which are based on the axial and tangential velocities upstream of the quarl. This allows to operate the system with the same mass flows as in Sec. 5. Experiments are only conducted here for the axial swirling vane yielding the highest swirl number $S_1 = 0.87$ in the central fuel stream. This corresponds to configurations where stable flames could easily be lifted with a straight injector. Injectors with three quarl angles in the annular stream were tested with $\alpha = 5$ deg, 10 deg, and 20 deg.

The results are compared to the straight annular injector with $\alpha = 0$ deg in Fig. 10. Only the Abel deconvoluted OH* intensity emission is presented for nine selected flames. The same topologies as in Fig. 5 can be identified when J, S_2 and S_1 vary. The transition between Type B and Type C flame is observed for different values of the quarl angle α depending on the values taken by J and S_2. This transition is plotted in Fig. 11 with respect to J and S_2 for the four values of the quarl angle α. When the quarl increases, the liftoff height decreases and the flame remains attached to the central fuel nozzle lip for a wider range of operating conditions. Along with the outer swirl number S_2 and the momentum flux ratio J, increasing the quarl angle α therefore reduces the liftoff height and strongly promotes flame attachment.

It is worth examining whether the impact of the quarl angle α can be explained by the evolution of J or S_2 through the change of cross section area of the annular nozzle. First, it is clear that the axial velocity u_{z_2} of the oxidizer stream decreases in the annular diffuser while the axial velocity u_{z_1} of the fuel inside the straight central tube remains unaltered. This, for example, leads to a drastic decrease in the momentum flux ratio J of about 60% when the quarl angle is set to $\alpha = 10$ deg compared to a straight injector. Second, it has been shown in Ref. [33] that the swirl number can not increase when passing through a diverging cup. Increasing the quarl angle α either decreases the swirl number when pressure terms are included in its definition, or it leaves the pressure less swirl number S_2 unaltered when effects of pressure are discarded. As a conclusion, increasing the quarl angle α barely changes the outer swirl number S_2, but leads to a decrease in the momentum flux ratio J.

It has been shown that decreasing J largely promotes flame detachment and increases the liftoff height. As the opening of the quarl angle rather provokes flame attachment, its impact on flame stabilization and flame topology in Fig. 10 cannot therefore be correlated with changes of J and S_2. This makes the quarl angle α a new independent parameter to control the flame liftoff, as already demonstrated for premixed flames in Ref. [33]. Its impact is interpreted as follows. Flame attachment observed in Figs. 10 and 11 is attributed to a lower position of the leading stagnation point of the CRZ. When the swirling jet angle widens thanks to an increase in the quarl angle α, the adverse pressure gradient in the quarl increases diminishing the height of the stagnation point [33]. The position of the flame leading edge lying close to this stagnation point of the CRZ is therefore lowered.

Fig. 11 Transition between Type B and Type C topology as sketched in Fig. 8, mapped with respect to the momentum flux ratio J and the outer swirl number S_2 for different quarl angles $\alpha = 0$ deg, 5 deg, 10 deg, and 20 deg. The inner swirl number is set to S_1 0.87.

Fig. 12 OH* flame images as a function of the mass fraction of oxygen in the annular stream $Y_{O_2,2}$ for two selected values of the momentum flux ratio J and the outer swirl number S_2. Images are deconvoluted with the Abel transform. The inner swirl number is set to S_1 0.87.

Fig. 13 Transition between Type B and Type C topology as sketched in Fig. 7, mapped with respect to the momentum flux ratio J and the outer swirl number S_2 for different level of oxygen enrichment $Y_{O_2,2}$. The inner swirl number is set to S_1 0.87.

7 Effect Oxygen Enrichment on Flame Topology

So far, only the aerodynamic characteristics of the flow inside the combustion chamber were modified. It is finally worth exploring the effects of chemistry with the help of a Damköhler number. This number is varied by modifying the level of oxygen enrichment in the annular stream. The impact of the O_2 enrichment on flame topology is analyzed with OH* deconvoluted images in Fig. 12 and with a stabilization regime map in Fig. 13. As in Sec. 6, experiments are reported for a fixed inner swirl number $S_1 = 0.87$. The oxygen mass fraction $Y_{O_2,2}$ ranges from 0.23, corresponding to an air mixture, to 0.5. For a fixed momentum flux ratio J, increasing $Y_{O_2,2}$ leads to a reduction of the global equivalence ratio. It appears that the flames feature the same topologies and the same type of stabilization modes as reported in Fig. 8. When the oxygen enrichment increases, the liftoff height reduces and the flames are more difficult to detach from the injector rim. As depicted in Fig. 13, transition from Type B to type C flames depends on $Y_{O_2,2}$. When the O_2 mass fraction is lower than $Y_{O_2,2} = 0.30$, all the reported flames are lifted. Conversely, when it is increased to $Y_{O_2,2} = 0.50$, only the flames with a moderate annular swirl S_2 and a high momentum flux in the inner fuel stream are lifted. Between these two limits, the mass fraction $Y_{O_2,2} = 0.40$ yields the best delineation between the lifted and the attached regimes. This oxygen enrichment allows to easily characterize the transition from Type B to type C regimes for a large range of combinations of J and S_2. This property has motivated the choice in this study to conduct the major part of the experiments at this level of O_2 enrichment.

Further experiments, not reported here, were also conducted at different levels of O_2 enrichment, but without inner swirl $S_1 = 0$. These flames are all attached to the nozzle rim, except a few flames with air as the oxidizer. All these experiments confirm that adding a swirl motion S_1 to the inner fuel stream confers a high flexible capacity to lift the flame, independently from the O_2 enrichment in the annular flow.

8 Conclusion

The impact of swirl on the stabilization of non premixed oxygen enriched flames has been investigated above a coaxial injector. In this system, methane is injected in the inner stream which is eventually put in rotation by an axial swirling vane. An oxidizing O_2/N_2 mixture composed of 40% of oxygen in mass flows into a swirling annular stream generated by an axial plus tangential device. Flame topologies stabilized above this injector have been investigated with OH* chemiluminescence images.

It has been shown that flame attachment and flame liftoff height mainly depend on the momentum flux ratio $J = \rho_2 u_{z,2}^2 / \rho_1 u_{z,1}^2$.
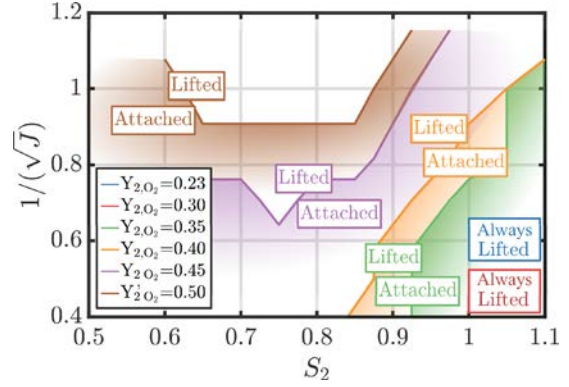
When the momentum flux ratio J is small, the flame is lifted and the liftoff height is maximum. Increasing J progressively reduces the liftoff height until the flames anchor to the rim of the central injector. This dimensionless number, disregarded in many studies in which the coflow velocity remains small, is here varied from $J = 0.75$ to 8 and used systematically to interpret the flame topologies observed above the injector.

It has been found that swirling the annular oxidizer stream or the inner fuel stream yield opposite effects. Without inner swirl $S_1 = 0$, flames could not be lifted over the range of operating conditions covered in this study. A major finding of this work is that when the central fuel stream is impregnated with swirl $S_1 > 0$, lifted flames with a stable central recirculating zone could be reached over a wide set of operating conditions. In this case, flame stabilization and liftoff characteristics have been found to depend on the inner swirl level S_1, the outer swirl level S_2 and the momentum ratio J between the two streams. Increasing the tangential outer momentum in the annular channel by increasing the outer swirl number S_2 or decreasing the inner axial momentum flux in the central tube by increasing the momentum flux ratio J lowers the position of the recirculating bubble and favors flame attachment to the central injector rim. Conversely, increasing the tangential inner momentum by increasing the inner swirl level S_1 or increasing the inner axial momentum by lowering the momentum flux ratio J favors flame detachment from the central injector rim.

Changes of the flame topology have been classified in four successive categories depicting the apparition and the position of distinct reaction layers in the flow as the inner swirl level increases. These four topologies largely impact the thermal stress to the injector and the flame compactness. Transitions from one topology to the following follow a similar pathway when S_1, S_2, and J are modified. These topologies have also been found to be not altered by the combustion chamber sidewalls. This proves that flame stabilization above this injector is not impaired by the presence of outer recirculation zones or by the gas composition of the external entrained flow.

The impact of a diverging cup placed at the outlet of the oxidizer stream has also been characterized. Increasing the quarl angle of the annular nozzle has been shown to greatly alter the flame topology by decreasing the flame liftoff height and promoting flame attachment to the central injector nozzle. Increasing the quarl angle lowers the position of the stagnation point of the central recirculating bubble. This leads to reduced flame liftoff heights independently from the swirl levels in the central and annular streams and the momentum ratio between these streams. These experiments confirm that a quarl is an independent control parameter to adjust flame liftoff.

Finally, the effects of mixture reactivity have been analyzed by changing the level of oxygen in the oxidizer annular stream. When the O_2 enrichment increases, lifted non premixed flames can be stabilized downstream coaxial injectors by increasing S_1 or decreasing S_2 or J. The main parameters allowing to control the liftoff height have therefore been identified. In particular, it has been shown that the use of the inner swirl yields both compact and lifted flames. The lifted flame regime is interesting from an industrial perspective to reduce the size of the equipment while limiting the thermal stress to the injector nozzle. These experiments were conducted with a coaxial injector in which the annular oxidizer velocity is not small compared to the central fuel jet velocity that is typical of many industrial injectors.

Acknowledgment

References

[1] De Persis, S., Foucher, F., Pillier, L., Osorio, V., and Gökalp, I., 2013, "Effects of O_2 Enrichment and CO_2 Dilution on Laminar Methane Flames," Energy, **55**, pp. 1055–1066.

[2] Baukal, C. E., and Gebhart, B., 1997, "Oxygen-Enhanced/Natural Gas Flame Radiation," Int. J. Heat Mass Transfer, **40**(11), pp. 2539–2547.

[3] Cieutat, D., Sanchez-Molinero, I., Tsiava, R., Recourt, P., Aimard, N., and Prébendé, C., 2009, "The Oxy-Combustion Burner Development for the CO_2 Pilot at Lacq," Energy Procedia, **1**(1), pp. 519–526.

[4] Toftegaard, M. B., Brix, J., Jensen, P. A., Glarborg, P., and Jensen, A. D., 2010, "Oxy-Fuel Combustion of Solid Fuels," Prog. Energy Combust. Sci., **36**(5), pp. 581–625.

[5] Ivernel, A., and Vernotte, P., 1979, "Etude Expérimentale de L'amélioration Des Transferts Convectis Dans Les Fours Par Suroxygénation du Comburant," Rev. Gener. Therm., **18**(210–211), pp. 375–391.

[6] Samaniego, J., Labegorre, B., Egolfopoulos, F., Ditaranto, M., Sautet, J., and Charon, O., 1998, "Mechanism of Nitric Oxide Formation in Oxygen-Natural Gas Combustion," Symp. (Int.) Combust., **27**(1), pp. 1385–1392.

[7] Chen, R., and Axelbaum, R., 2005, "Scalar Dissipation Rate at Extinction and the Effects of Oxygen-Enriched Combustion," Combust. Flame, **142**(1–2), pp. 62–71.

[8] Boushaki, T., Sautet, J., Salentey, L., and Labegorre, B., 2007, "The Behaviour of Lifted Oxy-Fuel Flames in Burners With Separated Jets," Int. Commun. Heat Mass Transfer, **34**(1), pp. 8–18.

[9] Yon, S., and Sautet, J.-C., 2012, "Flame Lift-Off Height, Velocity Flow and Mixing of Hythane in Oxy-Combustion in a Burner With Two Separated Jets," Appl. Therm. Eng., **32**, pp. 83–92.

[10] Peters, N., and Williams, F. A., 1983, "Liftoff Characteristics of Turbulent Jet Diffusion Flames," AIAA J., **21**(3), pp. 423–429.

[11] Vanquickenborne, L., and Van Tiggelen, A., 1966, "The Stabilization Mechanism of Lifted Diffusion Flames," Combust. Flame, **10**(1), pp. 59–69.

[12] Kalghatgi, G., 1984, "Lift-Off Heights and Visible Lengths of Vertical Turbulent Jet Diffusion Flames in Still Air," Combust. Sci. Technol., **41**(1–2), pp. 17–29.

[13] Ko, Y., and Chung, S., 1999, "Propagation of Unsteady Tribrachial Flames in Laminar Non-Premixed Jets," Combust. Flame, **118**(1–2), pp. 151–163.

[14] Buckmaster, J., 1996, "Edge-Flames and Their Stability," Combust. Sci. Technol., **115**(1–3), pp. 41–68.

[15] Karami, S., Hawkes, E. R., Talei, M., and Chen, J. H., 2016, "Edge Flame Structure in a Turbulent Lifted Flame: A Direct Numerical Simulation Study," Combust. Flame, **169**, pp. 110–128.

[16] Su, L., Sun, O., and Mungal, M., 2006, "Experimental Investigation of Stabilization Mechanisms in Turbulent, Lifted Jet Diffusion Flames," Combust. Flame, **144**(3), pp. 494–512.

[17] Lyons, K. M., 2007, "Toward an Understanding of the Stabilization Mechanisms of Lifted Turbulent Jet Flames: Experiments," Prog. Energy Combust. Sci., **33**(2), pp. 211–231.

[18] Brown, C. D., Watson, K. A., and Lyons, K. M., 1999, "Studies on Lifted Jet Flames in Coflow: The Stabilization Mechanism in the Near-and Far-Fields," Flow, Turbul. Combust., **62**(3), pp. 249–273.

[19] Guiberti, T., Boyette, W., Roberts, W., and Masri, A., 2018, "Pressure Effects and Transition in the Stabilization Mechanism of Turbulent Lifted Flames," Proc Combust. Inst., **37**(2), pp. 2167–2174.

[20] Yuasa, S., 1986, "Effects of Swirl on the Stability of Jet Diffusion Flames," Combust. Flame, **66**(2), pp. 181–192.

[21] Kim, H. K., Kim, Y., Lee, S. M., and Ahn, K. Y., 2006, "Emission Characteristics of the 0.03 mw Oxy-Fuel Combustor," Energy Fuels, **20**(5), pp. 2125–2130.

[22] Kim, H. K., Kim, Y., Lee, S. M., and Ahn, K. Y., 2007, "Studies on Combustion Characteristics and Flame Length of Turbulent Oxy-Fuel Flames," Energy Fuels, **21**(3), pp. 1459–1467.

[23] Chigier, N. A., and Beeŕ, J. M., 1964, "Velocity and Static-Pressure Distributions in Swirling Air Jets Issuing From Annular and Divergent Nozzles," J. Basic Eng., **86**((4), pp. 788–796.

[24] Chen, R.-H., and Driscoll, J. F., 1989, "The Role of the Recirculation Vortex in Improving Fuel-Air Mixing Within Swirling Flames," Proc. Combust. Inst., **22**(1), pp. 531–540.

[25] Feikema, D., Chen, R.-H., and Driscoll, J. F., 1990, "Enhancement of Flame Blowout Limits by the Use of Swirl," Combust. Flame, **80**(2), pp. 183–195.

[26] Degeneve, A., Vicquelin, R., Mirat, C., Labegorre, B., Jourdaine, P., Caudal, J., and Schuller, T., 2019, "Scaling Relations for the Length of Coaxial Oxy-Flames With and Without Swirl," Proc. Combust. Inst., **37**(4), pp. 4563–4570.

[27] Syred, N., Chigier, N., and Beer, J., 1971, "Flame Stabilization in Recirculation Zones of Jets With Swirl," Symp. (Int.) Combust., **13**(1), pp. 617–624.

[28] Chen, R.-H., Driscoll, J. F., Kelly, J., Namazian, M., and Schefer, R., 1990, "A Comparison of Bluff-Body and Swirl-Stabilized Flames," Combust. Sci. Technol., **71**(4–6), pp. 197–217.

[29] Truelove, J., Wall, T., Dixon, T., and Stewart, I. M., 1982, "Flow, Mixing and Combustion Within the Quarl of a Swirled, Pulverised-Coal Burner," Symp. (Int.) Combust., **19**(1), pp. 1181–1187.

[30] Dixon, T., Truelove, J., and Wall, T., 1983, "Aerodynamic Studies on Swirled Coaxial Jets From Nozzles With Divergent Quarls," ASME J. Fluids Eng., **105**(2), pp. 197–203.

[31] Mahmud, T., Truelove, J., and Wall, T., 1987, "Flow Characteristics of Swirling Coaxial Jets From Divergent Nozzles," ASME J. Fluids Eng., **109**(3), pp. 275–282.

[32] Jourdaine, P., Mirat, C., Caudal, J., and Schuller, T., 2018, "Stabilization Mechanisms of Swirling Premixed Flames With an Axial-Plus-Tangential Swirler," ASME J. Eng. Gas Turbines Power, **140**(8), p. 081502.

[33] Degeneve, A., Jourdaine, P., Mirat, C., Caudal, J., Vicquelin, R., and Schuller, T., 2019, "Effects of a Diverging Cup on Swirl Number, Flow Pattern and Topology of Premixed Flames," ASME Paper No. GT2018-76152.

[34] Otsu, N., 1979, "A Threshold Selection Method From Gray-Level Histograms," IEEE Trans. Syst., Man, Cybern., **9**(1), pp. 62–66.

[35] Wang, Q., Hu, L., Zhang, X., Zhang, X., Lu, S., and Ding, H., 2015, "Turbulent Jet Diffusion Flame Length Evolution With Cross Flows in a Sub-Pressure Atmosphere," Energy Convers. Manage., **106**, pp. 703–708.

[36] Villermaux, E., and Rehab, H., 2000, "Mixing in Coaxial Jets," J. Fluid Mech., **425**, pp. 161–185.

[37] Schumaker, S. A., and Driscoll, J. F., 2009, "Coaxial Turbulent Jet Flames: Scaling Relations for Measured Stoichiometric Mixing Lengths," Proc. Combust. Inst., **32**(2), pp. 1655–1662.

[38] Fanaca, D., Alemela, P., Hirsch, C., and Sattelmayer, T., 2010, "Comparison of the Flow Field of a Swirl Stabilized Premixed Burner in an Annular and a Single Burner Combustion Chamber," ASME J. Eng. Gas Turbines Power, **132**(7), p. 71502.

[39] Mongia, H., 2011, "Engineering Aspects of Complex Gas Turbine Combustion Mixers Part I : High Delta-T," AIAA Paper No. 2011–107.

[40] Juniper, M. P., 2001, "Structure and Stabilization of Cryogenic Spray Flames," Ph.D. thesis, Ecole Centrale de Paris, Paris, France.

[41] Tay-Wo-Chong, L., Komarek, T., Zellhuber, M., Lenz, J., Hirsch, C., and Polifke, W., 2009, "Influence of Strain and Heat Loss on Flame Stabilization in a Non-Adiabatic Combustor," European Combustion Meeting, Chania, Greece.

[42] Guiberti, T., Durox, D., Scouflaire, P., and Schuller, T., 2015, "Impact of Heat Loss and Hydrogen Enrichment on the Shape of Confined Swirling Flames," Proc. Combust. Inst., **35**(2), pp. 1385–1392.